Supplemental material

Ren et al., https://doi.org/10.1083/jcb.201808131

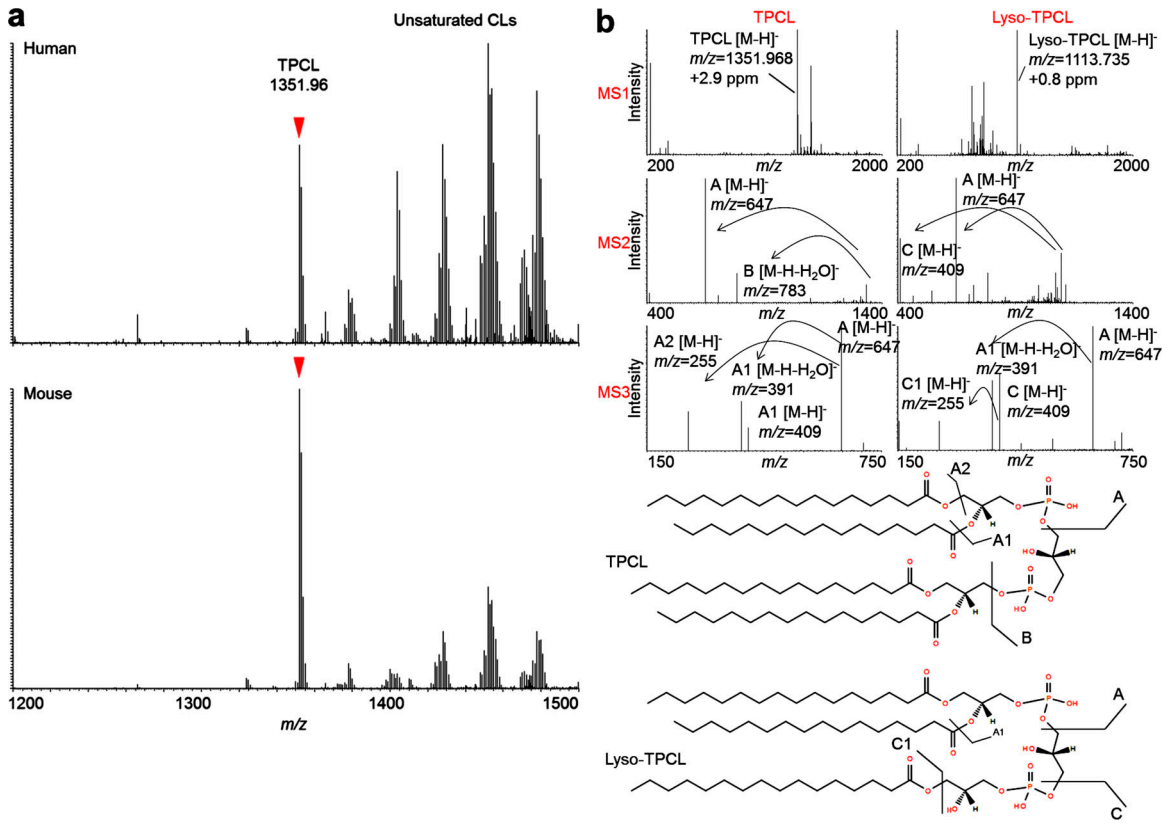

Figure S1. **TPCL is present in the testes of humans and mice. (a)** Lipid extracts from testes were analyzed by LC-MS/MS by using an LTQ Orbitrap coupled to a C8 reversed-phase column. The depicted MS1 subspectra were acquired over 2 min during the elution of TPCL. **(b)** Lipid extracts from mouse testes were analyzed by MSn by using an LTQ Orbitrap coupled to a C8 reversed-phase column. The MS1 spectra were acquired over 1 min during the elution of TPCL and lyso-TPCL, respectively. The MS2 spectra were acquired of the m/z = 1,352.0 and m/z = 1,113.7 ions, respectively. The MS3 spectra were acquired of the m/z = 647 and m/z = 409 ions, respectively. The fragment ions are shown in the chemical structures underneath the spectra.

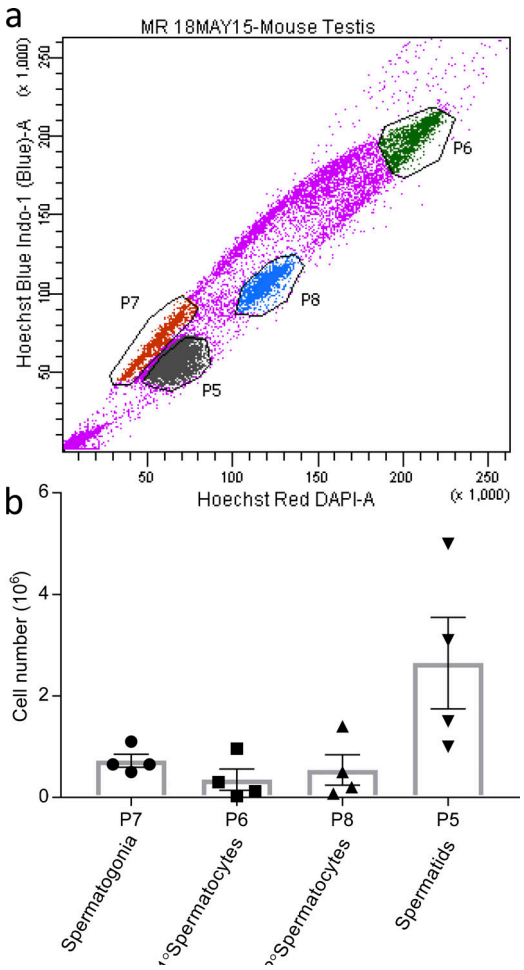

Figure S2. **Separation of germ cells by flow cytometry.** Adult mouse testes were dissected and treated with collagenase and with trypsin. Dissociated cells were stained with Hoechst and separated by fluorescent-activated cell sorting. **(a)** Representative scatter plot indicating the main germ cell fractions. **(b)** Bar graph showing the yield of the germ cell fractions from four independent experiments.

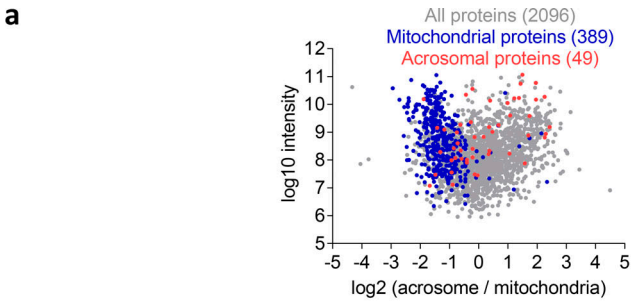

Protein	ID	Abundance ratio acrosome/mitochondria
Aminomethyltransferase, mitochondrial	Amt	5.07
Sperm mitochondrial-associated cysteine-rich protein	Smcp*	4.44
Sulfite oxidase, mitochondrial	Suox*	3.35
Mitochondria-eating protein	Spata18*	2.63
Glycine dehydrogenase (decarboxylating), mitochondrial	Gldc*	2.31
Aspartate aminotransferase, mitochondrial	Got2	1.88
Probable D-lactate dehydrogenase, mitochondrial	Ldhd	1.59
Alpha-aminoadipic semialdehyde synthase, mitochondrial	Aass	1.33
Mitochondrial thiamine pyrophosphate carrier	Slc25a19*	1.29
NADH dehydrogenase [ubiquinone] iron-sulfur protein 6	Ndufs6	1.11

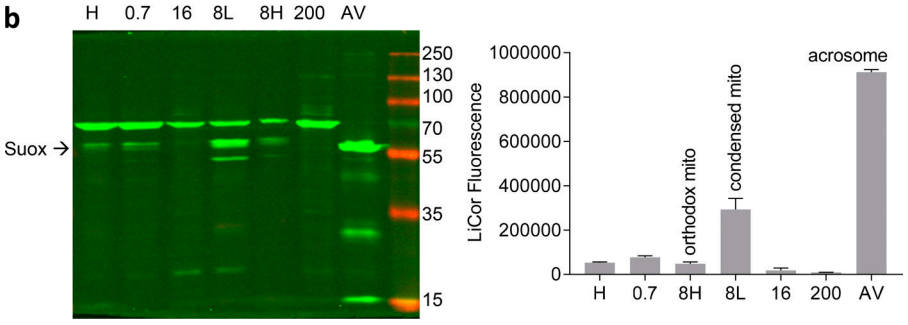

Figure S3. **Mitochondrially annotated proteins are present in the acrosome. (a)** Mitochondria were purified from testis homogenate. Acrosomal vesicles were released from sperm by the acrosome reaction. The organelles were analyzed by quantitative proteomics by using TMTs. Logarithmic MS1 signal intensities were plotted against the logarithmic ratio of the MS2-based intensities of the acrosome tag over the mitochondria tag. The table lists proteins for which the acrosome/mitochondria ratio was >1. Proteins marked with an asterisk were specifically associated with condensed mitochondria. **(b)** Subcellular fractions were prepared from testis homogenate (H) by centrifugation at 700 *g* (0.7), 8,000 *g* (8), 16,000 *g* (16), and 200,000 *g* (200). The 8,000-*g* pellet was separated into a high-density (8H) and a low-density (8L) fraction by Percoll gradient. Acrosomal vesicles (AV) were released from sperm by the acrosome reaction. Aliquots (75 µg of protein) were analyzed by quantitative Western blotting with an antibody to Suox by using the LiCor system. Full-length Suox was identified based on its predicted mass (61 kD). Suox was present in mitochondria and in acrosomes. Acrosomal Suox appeared to be partially degraded. Bar graphs show mean values with ranges of two independent measurements.

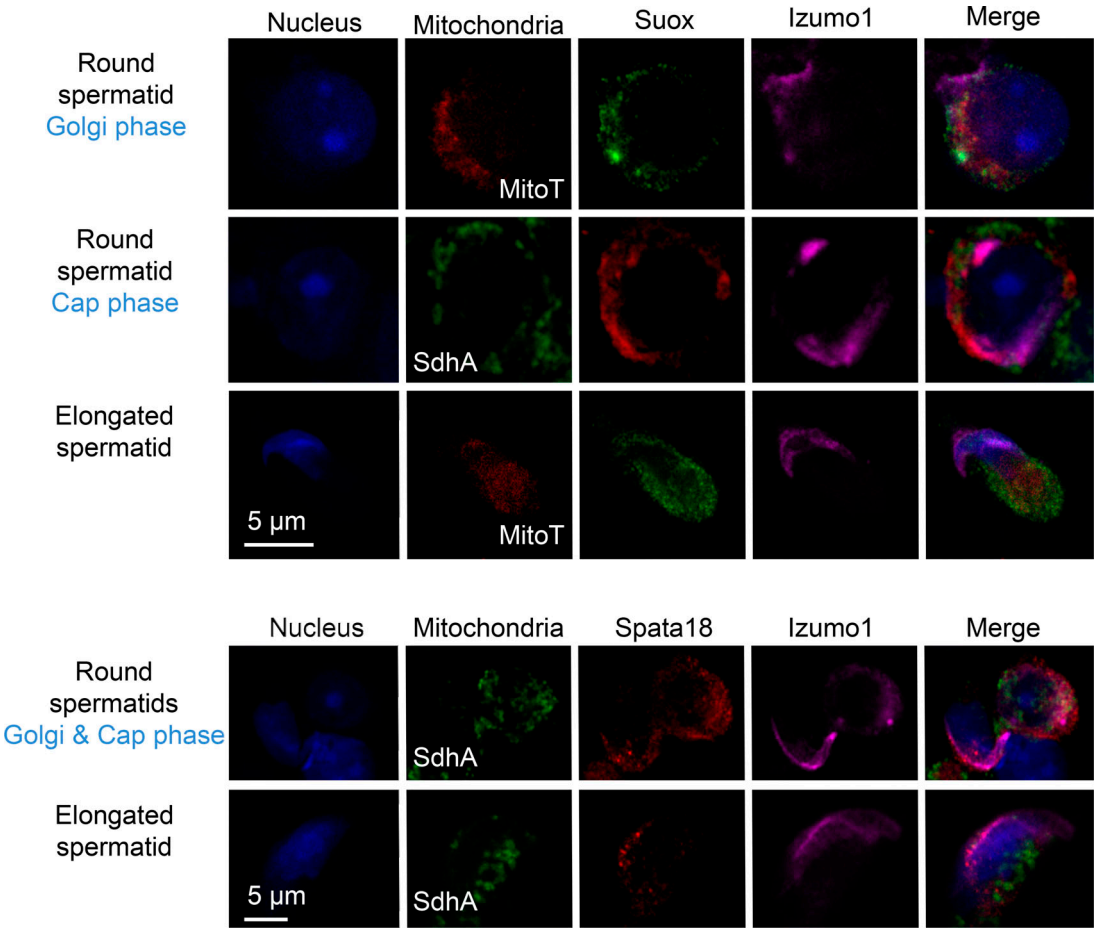

Figure S4. **Suox and Spata18 merge with the nascent acrosome in the Golgi phase and remain associated with the acrosome during spermatid development.** Round spermatids were analyzed by immunofluorescence by using antibodies to Suox, Spata18, and Izumo1 (acrosome marker) and the SdhA subunit of respiratory complex II. The nucleus was stained with Hoechst dye. In some experiments, mitochondria were visualized with MitoTracker (MitoT) instead of SdhA.

Provided online are three tables in Excel. Table S1 lists data from affinity purification experiments. Table S2 lists the lipid composition of acrosomal membranes. Table S3 lists CL molecular species in mitochondria and LNMs from mouse testis.